Landsc Ecol (2023) 38:2501–2518
https://doi.org/10.1007/s10980-023-01710-1

RESEARCH ARTICLE

Proportion of forest area burned at high-severity increases with increasing forest cover and connectivity in western US watersheds

Emily J. Francis · Pariya Pourmohammadi · Zachary L. Steel · Brandon M. Collins · Matthew D. Hurteau

Received: 7 October 2022 / Accepted: 26 June 2023 / Published online: 8 July 2023

Abstract

Context In western US forests, the increasing frequency of large high-severity fires presents challenges for society. Quantifying how fuel conditions influence high-severity area is important for managing risks of large high-severity fires and understanding how they are changing with climate change. Fuel availability and heterogeneity influence high-severity fire probability, but heterogeneity is insensitive to some aspects of forest connectivity that are important to potential high-severity fire transmission and thus high-severity area.

Objectives To quantify the effects of fuel availability, heterogeneity, and connectivity on the proportion of forest area burned at high-severity (high-severity burn area). To use the extreme 2020 fire season to consider how climate change could affect high-severity burn area relationships.

Methods We used datasets derived from remote sensing to quantify effects of forest fuel availability, heterogeneity, and connectivity on extreme (95th percentile) high-severity burn areas in western US coniferous watersheds from 2001 to 2020. We developed a connectivity metric to quantify potential high-severity fire transmission.

Results High-severity burn area increased with increasing fuel availability and connectivity and decreased with increasing heterogeneity. In 2020, multiple large high-severity burn areas occurred in forests with high fuel availability, which only had small high-severity burn areas prior to 2020.

Conclusions In forests with an annual fire season, management to limit forest connectivity and fuel accumulation and increase heterogeneity could mitigate the potential for large high-severity fires. In forests where climate usually limits fire, large high-severity fires may occur more frequently if climate change increases the frequency of years with inadequate climatic barriers to wildfire.

Keywords Wildfire · Climate change · Forest structure · Disturbance · Connectivity · Continuity

Supplementary Information The online version contains supplementary material available at https://doi.org/10.1007/s10980-023-01710-1.

E. J. Francis (✉) · M. D. Hurteau
Department of Biology, University of New Mexico, Albuquerque, NM, USA
e-mail: emilyfrancis1@unm.edu

P. Pourmohammadi
Planet Labs, San Francisco, CA, USA

Z. L. Steel
USDA Forest Service, Rocky Mountain Research Station, Fort Collins, CO, USA

B. M. Collins
Department of Environmental Science, Policy, and Management, University of California–Berkeley, Berkeley, CA, USA

Introduction

Fire is a fundamental natural disturbance process in forest ecosystems (Agee and Skinner 2005; Bowman et al. 2009; McLaughlan et al. 2020) that can provide multiple ecosystem services (Pausas and Keeley 2019). However, in the western US, climate change and past management have altered forest fire regimes (Agee and Skinner 2005; Abatzoglou and Williams 2016; Hessburg et al. 2021). Fire suppression has reduced fire frequency which, coupled with increased fuel aridity driven by climate change, has led to increasing forest area burned and increasing fire severity (Abatzoglou and Williams 2016; North et al. 2021; Juang et al. 2022). The area burned at high-severity in western North American forests has increased eightfold since 1985 (Parks and Abatzoglou 2020) and there is evidence from coniferous forests in California that the size of high-severity fire patches is increasing (Stevens et al. 2017; Steel et al. 2018). Increasingly frequent high-severity fire has widespread impacts to forest ecosystem services and society, including higher risks of post-fire forest conversion to shrubland (Coop et al. 2020), challenges to water resources management (Bladon et al. 2014; Rhoades et al. 2019), and public health impacts associated with wildfire smoke exposure (Liu et al. 2016; Stowell et al. 2019; Burke et al. 2021).

The potential forest area burned at high-severity is a function of weather, topography, climate, and the amount and arrangement of fuel (Littell et al. 2009). Regionally, climate is an important determinant of forest flammability and locally, forest structure, fuel availability, weather, and topography influence wildfire behavior and severity (Agee and Skinner 2005). In climate-limited systems, cool and wet conditions inhibit wildfire ignition and spread most years, causing long periods between fire events and an accumulation of biomass. In systems that have an annual fire season, known as fuel-limited systems, conditions during the fire season are almost always conducive to burning and fuel availability and structure determine flammability (Krawchuk and Moritz 2011; Steel et al. 2015; Pausas and Paula 2012). However, the lack of recent fire in these fuel-limited systems, owing to fire suppression and exclusion policies, allowed for uncharacteristically high fuel accumulations, which increases flammability (Stephens and Fulé 2005; Hagmann et al. 2021).

Fuel availability, forest heterogeneity, and forest connectivity influence fire behavior and fire severity in different ways. Fuel availability, or the amount of fuel at a single location, has a strong influence on the probability of high-severity fire at that location (Parks et al. 2018; Koontz et al. 2020). In previous studies, remotely-sensed vegetation indices including the normalized difference vegetation index (NDVI) have been used as proxies for fuel availability (Parks et al. 2018; Koontz et al. 2020). Forest heterogeneity in the neighborhood surrounding a location influences the probability of high-severity fire at that location (Koontz et al. 2020; Steel et al. 2021). Standard deviation in either NDVI or vegetation cover (Steel et al. 2021) within a neighborhood surrounding a location have been used in recent studies to quantify forest heterogeneity. At the neighborhood or local scale that has been used in these studies, greater forest heterogeneity in the neighborhood surrounding a location may correspond to discontinuity in fuel availability (Koontz et al. 2020) and therefore provide a way to quantify forest connectivity. However, it may be an indirect measure of fuel connectivity in larger neighborhoods, i.e., landscapes because it is insensitive to the spatial arrangement of fuels within the landscape. A landscape with high fuel availability in half of its total area and low fuel availability in the remaining half of its area would have high fuel heterogeneity, but depending on the spatial arrangement of the locations with low and high fuel availability, the expected fire behavior and thus high-severity fire probability could differ. For example, if the landscape consisted of two large patches—one with low fuel availability and one with high fuel availability—we would expect that high-severity fire would be more likely to propagate across the entire patch of high fuel availability. On the other hand, If the landscape consisted of a checkerboard pattern, where locations with low and high fuel availability were adjacent to each other but locations with high fuel availability were rarely or never adjacent, we would expect that high-severity fire in one location with high fuel availability would be less likely to be transmitted to the other locations with high fuel availability, resulting in a lower proportion of area burned at high severity (Hessburg et al. 2015, 2021). This is an example of two forest landscapes with equivalent heterogeneity, but different forest connectivity (SI Figures Fig. S1) that would be expected to result in different fire behavior,

transmission, and severity patterns. Characterizing the spatial patterns of fuels is critical for determining the scale at which fuel heterogeneity influences fire severity (Koontz et al. 2020). While fine-scale heterogeneity in fuels may slow or stop the spread of low intensity surface fire (e.g., Jaffe et al. 2021), more extreme fire behavior (wind-driven, plume-driven, mass fire, and long ember transport) likely requires much larger areas of reduced fuel to slow or stop fire spread (Koo et al. 2010; Prichard et al. 2020; Stephens et al. 2022).

Management can manipulate forest connectivity, fuel availability, and heterogeneity to reduce the transmission of high-severity fire across forest landscapes (North et al. 2021). However, understanding where fuel conditions are in a condition of high risk for the transmission of high-severity fire is important for managing them. In this study, we investigated how the availability, connectivity, and heterogeneity of forest cover relates to high-severity burned area at the watershed scale in all coniferous watersheds across the western United States over the last two decades (2001–2020). We used the mean percent forest cover of forested areas as a proxy for fuel availability and the standard deviation in forest canopy cover within forested locations as a proxy for fuel heterogeneity. We quantified forest connectivity using a set of landscape pattern metrics from the FRAGSTATS program, and also developed a new connectivity metric to quantify the proportion of the forest area that would be susceptible to high-severity crown fire if high-severity crown fire was present in any single forest pixel. We used previously established representations of forest cover to calculate these proxies for "fuels" given their comprehensive coverage and relatively high fidelity (Zhu et al. 2006). We expected the influence of fuels on high-severity burn area to be strongest in fuel-limited, rather than climate-limited systems. However, given the widespread fire activity experienced in the 2020 fire year across both fuel-limited and climate-limited systems in the western US (Abatzoglou et al. 2021; Higuera and Abatzoglou 2020; Safford et al. 2022), we expected greater convergence in the relationship between fuels and high-severity burned area. To test this hypothesis, we compared fuel-high-severity burned area relationships from 2001 to 2020 with the same relationships excluding the 2020 fires. We used the observed changes in fuel-high-severity burn area relationships when including the 2020 fires to consider how high-severity burn area risk could change if historically climate-limited systems are exposed to weakened climatic barriers to wildfire with increasing frequency.

Methods

We analyzed fuel-high-severity burn area relationships in coniferous forest watersheds in the western US. We used the Hydrological Unit Code 12 (HUC-12) watersheds from the Watershed Boundary Dataset. The Watershed Boundary Dataset is a dataset produced by the USGS that outlines watersheds in the United States based on topographic and hydrologic features, using a nested system that divides the US into 21 HUC-2 watersheds, 222 HUC-4 watersheds, 370 HUC-6 watersheds, 2270 HUC-8 watersheds, and ~ 90,000 HUC-12 watersheds, based on a set of federal standards and procedures (U.S. Geological Survey and U.S. Department of Agriculture, Natural Resources Conservation Service 2013). We used HUC-12 watersheds as our unit of analysis, which range in size from 10,000 acres to 40,000 acres. The Watershed Boundary Dataset including the HUC-12 watersheds is available for public download at https://www.usgs.gov/national-hydrography/access-national-hydrography-products. To identify coniferous forest HUC-12 watersheds in the western US, we quantified coniferous forest cover within watersheds, and used the LANDFIRE Existing Vegetation Type (EVT) and Biophysical Settings (BpS) data products to calculate the proportion of pixels within the watershed that were non-flammable, developed or agricultural, and the proportion of vegetated pixels that were coniferous forest. We included watersheds if at least 75% of the pixels were flammable, no greater than 50% of pixels were developed or agricultural, and if at least 25% of the vegetated pixels were coniferous forest. From the BpS GROUPVEG classification, we considered the "Conifer", "Conifer-Hardwood," and "Peatland Forest" categories as coniferous forest. Based on this definition for a coniferous watershed, there were 11,962 HUC-12 watersheds in our dataset. However, there were 3493 fires in those watersheds during the study period, with the inclusion criteria detailed below. Therefore, we modeled relationships between fuel conditions and high-severity burn area in those 3493 fires in watersheds, and then assessed spatial

variability in the potential size of high severity burn areas by using the model to predict high-severity burn area on each of the 11,962 coniferous watersheds.

Quantifying pre-fire forest fuel availability, variability, and structure

We used LANDFIRE data to quantify pre-fire fuel characteristics within the predominantly coniferous HUC-12 watersheds. The LANDFIRE program provides a set of continuous spatial datasets that quantify a wide range of vegetation, disturbance and topographic attributes for land in the United States (Rollins 2009). LANDFIRE datasets were developed by using Landsat imagery, topographic data from the National Elevation Dataset (NED), soils data from the State Soil Geographic (STATSGO) database, and weather and topographic data to predict attributes measured in the LANDFIRE field-referenced database, an extensive set of geo-referenced sampling plots, using classification and regression tree algorithms (Zhu et al. 2006; Rollins 2009; Reeves et al. 2009). LANDFIRE datasets were originally developed using circa 2001 Landsat imagery, and the base maps were updated using circa 2016 Landsat imagery. LANDFIRE data is available for public download at www.landfire.gov.

To quantify forest fuel availability, connectivity, and heterogeneity within each HUC-12 watershed, we derived metrics from the LANDFIRE existing vegetation cover and canopy bulk density data products. We used these two data products because their reported prediction accuracy was reasonable enough to capture broad-scale variation—the R correlation coefficient for predicted versus observed canopy bulk density ranged from 0.45 to 0.85 across 12 LANDFIRE mapping zones and R^2 for forest canopy cover was 0.78 to 0.88 in two mapping zones (Zhu et al. 2006). To classify burnable and non-burnable cover for the quantification of the proportion non-burnable and forest connectivity by burnable cover, we used the LANDFIRE 40 Scott and Burgan Fire Behavior fuel model data product. All fuel models within the 40 Scott and Burgan 'nonburnable' fuel types were classified as non-burnable cover, including NB1: urban/developed, NB2: snow/ice, NB3: agricultural, NB8: open water, and NB9: barren (Scott and Burgan 2005).

We calculated five metrics of landscape composition (Gustafson 1998) that quantified fuel availability and variability, including mean forest canopy cover of forested pixels in the watershed, mean canopy bulk density of forested pixels in the watershed, and the proportion of pixels within the watershed that were not burnable as measures of fuel availability and standard deviation of canopy cover of forested pixels within the watershed and standard deviation of canopy bulk density of forested pixels within the watershed as measures of fuel variability (SI Tables Table S1). The existing vegetation cover data product classifies pixels within categories of tree cover—e.g. between 10 and 20% tree cover. To calculate mean canopy cover, we calculated the midpoint of the class (e.g. 15% canopy cover). As measures of landscape configuration (Gustafson 1998) or forest fuel structure, we used the existing vegetation cover to classify pixels as either forest or non-forest and calculated five separate metrics: edge density, patch density, proportion of like adjacency, forest connectivity by forest cover, and forest connectivity by burnable cover (SI Tables Table S1). Edge density is a measure of the length of the edges of a cover type as a fraction of the landscape area. Patch density is a measure of the number of patches of a cover type as a fraction of the landscape area. The proportion of like adjacency is the number of adjacencies between cells of a single cover type (like adjacencies) as a fraction of the total number of adjacencies between cells that involve that cover type, multiplied by 100. For both patch density and the proportion of like adjacency, a value is calculated for each cover type (forest and non-forest). We calculated patch density as the density of non-forested patches, and the proportion of like adjacency as the proportion of like adjacency of forested patches (McGarigal and Marks 1995). Edge density, patch density, and proportion of like adjacency were originally developed as part of the FRAGSTATS program, whereas forest connectivity by forest cover and forest connectivity by burnable cover were developed specifically for quantifying forest connectivity relevant to wildfire spread in this study. We developed the following metric of forest connectivity that quantifies the average proportion of forest area that would be susceptible to catching high-severity fire if any single forest pixel had high-severity crown fire, defined as:

$$\text{Forest Connectivity} = \frac{\frac{1}{N}\sum_{i=1}^{N} F_i}{F}$$

where forest connectivity is the area of forest connected to (i.e. in the same patch) as each individual forest pixel (F_i), averaged over all forest pixels in the watershed (N), as a proportion of the total forested area within the watershed (F). To understand the expected behavior of the metrics of landscape configuration (Neel et al. 2004), including the forest connectivity metric, we generated three hypothetical watersheds with varying forest cover patterns and calculated each metric of landscape configuration for each watershed (SI Figures Fig. S1). The forest connectivity metric approaches 1, when every forest pixel in the watershed is connected to 100% of the other forest pixels in the watershed (Fig. S1a), and has a minimum possible value of zero, which occurs when every forest pixel in the watershed is only adjacent to non-forest pixels within the watershed (Fig. S1c). We calculated forest connectivity by forest cover and forest connectivity by burnable cover. To calculate forest connectivity by forest cover, forest cells were only considered connected if they were connected by other forest cells, i.e. if they were part of a single patch of forest. To calculate forest connectivity by burnable cover, forest cells were considered connected if they were connected by any burnable cell types (i.e. if the forest cells were within a patch of burnable cell types, where burnable cell types included, but were not limited to, forest cells). For both forest connectivity by forest cover and by burnable cover, pixels were considered connected (i.e. in the same patch) if they shared a side, but those that were only connected on the diagonal were not (e.g. rook's neighborhood). The forest connectivity by forest cover metric is somewhat similar to the mean patch area of the forest class divided by the total class area of the forest class (where the mean patch area and total class area are each metrics from FRAGSTATS, McGarigal et al. 2012) with two key differences specific to wildfire behavior applications: (1) in the forest connectivity metric, the area of forest connected to each individual forest pixel (F_i) is the area of the patch minus the area of the one pixel, to calculate the remaining forest area that would be susceptible to catching high-severity wildfire if the focal pixel was on fire, and (2) mean patch area is calculated on a per pixel, rather than a per patch basis, in order to quantify the average proportion of remaining forest area that would be susceptible to catching high-severity wildfire if any individual pixel had high-severity wildfire. We used the landscape metrics R package to calculate edge density, patch density, and the proportion of like adjacency, and to delineate forest patches to calculate the number of cells connected to a focal cell for forest connectivity by forest cover and to delineate non-burnable patches for forest connectivity by burnable cover (Hesselbarth et al. 2019). Although cross-watershed wildfire transmission can occur, we calculated all metrics at the scale of the HUC-12 watershed.

We used the LANDFIRE base map data products from 2001 to 2016 to derive the fuel availability, variability, and structure characteristics (described above and in SI Tables Table S1 and shown in Fig. 1) that we used as predictor variables for high-severity burn area (as described below and shown in Fig. 1) of fires that occurred following the most recent base maps. Specifically, we used the data products from the 2001 base map to calculate the fuel predictor variables for fires that occurred between 2001 and 2015, and used the data products from the 2016 base map as predictor variables to calculate the fuel predictor variables for fires that occurred between 2016 and 2020.

In order to mitigate the effects of changes in fuel characteristics that occurred between the LANDFIRE Landsat imagery acquisition date (circa 2001 or circa 2016) and the date of subsequent fires (2001–2015 or 2016–2020), we did not include fires that burned over areas that had undergone significant disturbance due to fire in between the imagery acquisition date and the year of the fire. Specifically, if a fire burned over 45 hectares within a watershed, we did not include any subsequent fire that burned in that watershed prior to the update of the LANDFIRE data products with 2016 Landsat imagery, or if a fire burned over 45 hectares within a watershed after 2016, we did not include any subsequent fires in that watershed (because there has not been a new base map created since 2016). This reduced the effects of fire-watershed combinations in the analysis that burned over vegetation conditions that were likely to have been substantially altered by fire disturbances after the Landsat imagery was collected but prior to the fire.

Calculating high-severity burned area

We used fire perimeters from the Monitoring Trends in Burn Severity (MTBS) program for fires that occurred between 2001 and 2019, excluding fires

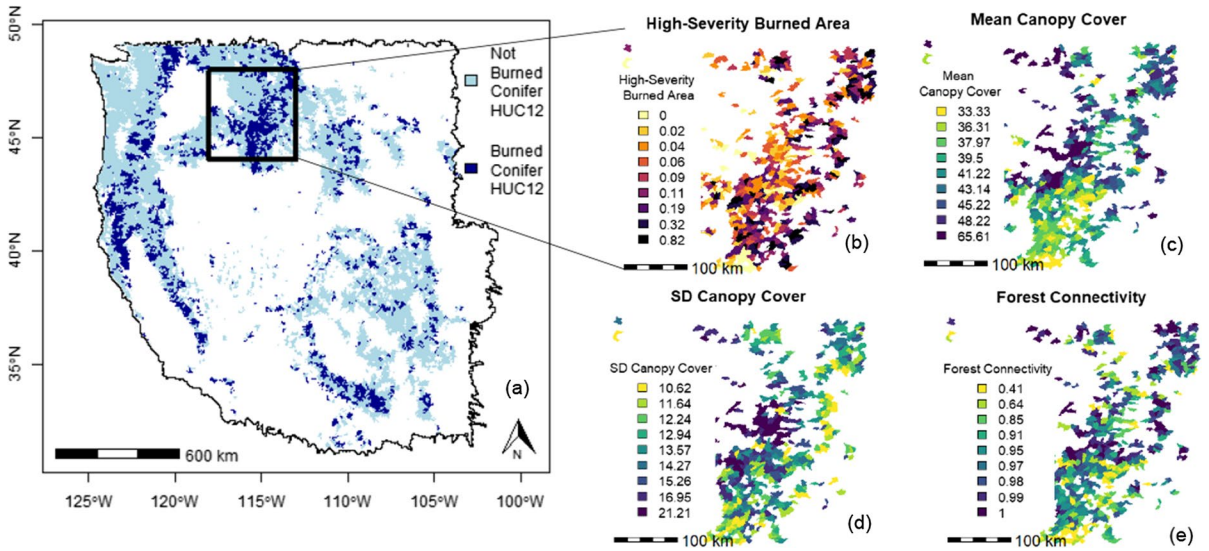

Fig. 1 Coniferous HUC-12 watersheds in the western US that burned between 2001 and 2020 and a subset of fuel predictor variables and the high-severity burned area response variable calculated for each burned watershed in a zoomed-in region. Light blue shading in panel (**a**) shows the 11,962 coniferous forest HUC-12 watersheds in the western US, and dark blue shading shows burned coniferous forest watersheds (coniferous forest watersheds with fires that occurred between 2001 and 2020 and burned over at least 10% of the total watershed area, SI Methods). Panels (**b**)–(**e**) show burned watersheds for a zoomed-in region of the Northern US Rockies, where (**b**) shows the proportion of forested area burned at high-severity, and panels (**c**)–(**e**) show a subset of the fuel predictor variables. In each panel, the axis legends show the upper boundary, rounded to two decimal places, of ten quantiles of each predictor variable, where the color of each watershed represents which of the ten quantiles of each variable it was within

that were classified as prescribed fires in the MTBS dataset (Eidenshink et al. 2007). MTBS is a program of the U.S. Department of Agriculture Forest Service and the U.S. Geological Survey that provides maps of fire extent and severity of large fires in the United States (Eidenshink et al. 2007) and is available for public download at www.mtbs.gov. In the western United States, MTBS maps fires that are at least 1000 acres equivalent to approximately 400 ha. MTBS data for western US wildfires were not yet available for 2020 fires at the time of this analysis, and we therefore used fire perimeters from the Fire Events Delineation (FIRED) dataset. FIRED is an algorithm and database that maps fire extents from the MODIS burned area product (Balch et al. 2020) and is available for download at https://scholar.colorado.edu/concern/datasets/8336h304x (St. Denis et al. 2022). A comparison between the size of individual MTBS and FIRED fire events suggested strong agreement between the two datasets ($R^2 = 0.92$, Balch et al. 2020). FIRED maps fires larger than 21 ha (Balch et al. 2020). To quantify burn severity within MTBS (2001–2019) and FIRED (2020) fire perimeters, we used an algorithm that predicts the Composite Burn Index (CBI) from multiple Landsat spectral indices, climate, and latitude from publicly-available data and Google Earth Engine code (Parks et al. 2019). To calculate high-severity burn area within each watershed, we calculated the proportion of the forested area in the watershed that burned at high-severity, where high-severity was defined as CBI $\geq$ 2.25, corresponding to stand-replacing fire and greater than 95% canopy mortality (Miller et al. 2009). The pre-fire forested area in the watershed for the calculation of the proportion of the forested area in the watershed burned at high-severity was determined from the LANDFIRE existing vegetation cover classification (forest vs. non-forest) data product. The distribution of watersheds that included any area burned contained a large proportion of watersheds in which only a small area of the watershed burned. We restricted the analysis to watershed-fire combinations in which at least 10% of the total area of the watershed burned, regardless of cover type. Hereafter we use the term

"high-severity burn area" to signify the proportion of the forested area in the watershed that burned at high-severity, as defined above.

Statistical analysis

Fires in watersheds where large forested areas within the watershed burned at high-severity occurred rarely (SI Figures Fig. S3), but have the largest consequences for forest ecosystem services and forest regeneration following wildfire (Coop et al. 2020). To focus on these rare but high-consequence events, we used quantile regression (Koenker and Bassett 1978; Koenker and Hallock 2001) to model the influence of fuel on the 95th percentile of proportion of the forested area in the watershed burned at high-severity, referred to as high-severity burn area throughout the manuscript. This approach of focusing on the potential for extreme outcomes by using quantile regression is analogous to an approach commonly used in fire behavior simulations, which often simulate wildfire behavior under the 90th or 97.5th percentile of weather conditions, in order to inform the design of fuel treatments that will be effective during extreme conditions (Stephens et al. 2009). In this study, we used statistical modeling rather than a simulation modeling approach, but were similarly focused on understanding what fuel conditions have the potential to lead to the most extreme outcomes. Quantile regression therefore allowed us to ask whether and how fuel characteristics affected the size of the extremes of forest area burned at high-severity. High-severity burn area is a proportion and was therefore bounded between 0 and 1. We used logistic quantile regression, appropriate for analysis of bounded outcomes, by we applying a logistic transformation to high-severity burn area prior to fitting the model (Bottai et al. 2010):

$$\text{logit}(\text{y}) = \log \frac{(\text{y} - y_{min})}{(y_{max} - \text{y})}$$

where y is the high-severity burn area (as defined in the "Methods" section 'Calculating High-Severity Burn Area'), y_{max} is the maximum possible high-severity burn area and is equal to 1, and y_{min} is the minimum possible high-severity burn area is equal to zero. A logistic transformation was used to account for the bounded nature of the data as explained in Bottai et al. (2010) and is commonly applied in studies that use quantile regression to model proportion data (e.g. Guo et al. 2021; Sofaer et al. 2022). All quantile regression analyses were done using the quantreg R package (Koenker 2018). All model predictions were back-transformed to yield predictions ranging from 0 to 1 (Bottai et al. 2010). Prior to quantile regression modeling, we used a min–max scalar to normalize all predictor variables to range from − 1 to 1. This normalization allowed us to interpret the model coefficients for each predictor variable as the change in high-severity burn area that would be expected from a change over half of the range of each of the predictor variables.

We modeled the data with and without the 2020 data because of the large number of fires that occurred in the Pacific Northwest during the 2020 fire season. Fire in this region of the country is often considered climate-limited and we sought to determine how that might alter the model. To determine whether to include quadratic terms for predictor variables in the model, we first inspected scatterplots of the relationships between each predictor variable and high-severity burn area in 2001–2019 and 2001–2020 (SI Figures Figs. S7, S8). If scatterplots suggested the presence of non-linearity that could be plausibly explained by an ecological process for either set of years, we included quadratic terms in the model for both sets of years (in order to prevent differences in model form between years from influencing our inferences about the differences between the two sets of years). Using this process, we included quadratic terms for mean canopy cover and the standard deviation in canopy cover. Scatterplots suggested a hump-shaped relationship between high-severity burn area and mean canopy cover from 2001 to 2019 (SI Figures Fig. S8), which could be explained by the intermediate fire-productivity hypothesis (Pausas and Paula 2012). For standard deviation in canopy cover, the non-linear relationship could be explained by the fact that watersheds with the lowest standard deviation in canopy cover may have been more likely to have lower canopy cover overall, corresponding to lower high-severity burn area. However, with increasing standard deviation in canopy cover, mean canopy cover and standard deviation in canopy cover were less likely to be coupled, and we expected the relationship between standard deviation in canopy cover and high-severity burn area to resemble the

relationship between heterogeneity in NDVI and probability of high-severity fire established by Koontz et al. (2020).

Many of the variables we calculated to describe fuel characteristics, particularly the variables that described forest fuel structure, calculated similar aspects of forest fuel structure and we anticipated that they could be correlated. To reduce multicollinearity among the predictor variables, we used an approach used by Dahlin et al. (2013). The steps of this approach are: (1) calculate the Pearson R correlation coefficient among all pairwise combinations of predictor variables, and (2) identify variable pairs with a Pearson R correlation coefficient greater than 0.5, (3) calculate the correlation between each variable within the correlated pair and the response variable independently, and (4) retain the predictor variable with the higher correlation with the dependent variable and remove the predictor variable with the lower correlation coefficient with the dependent variable. Because we used quantile regression, for step (3), we calculated the goodness-of-fit metric for quantile regression for the 95th percentile for the correlations between each individual with the pair of predictor variables, rather than the Pearson R correlation coefficient (Koenker and Machado 2012). To calculate quantile regression goodness of fit, we used the WRTDSTidal R package (Beck 2019). We simplified redundant predictor variables separately for models including 2001–2019 data and 2001–2020 data. After this step of excluding redundant predictor variables, we added an interaction term between mean canopy cover and forest connectivity by forest cover. The final form of the model was:

$$
\begin{aligned}
&Q_{high-severityburnarea}(\tau = 0.95|x) = \beta_0(\tau)\\
&+\beta_1 \text{ Mean Canopy Cover}(\tau)\\
&+\beta_2 \text{ Mean Canopy Cover}^2(\tau)\\
&+\beta_4 \text{ SD Canopy Cover}(\tau)\\
&+\beta_5 \text{ SD Canopy Cover}^2(\tau)\\
&+\beta_6 \text{ SD Canopy Bulk Density}(\tau)\\
&+\beta_8 \text{ Edge Density}(\tau)\\
&+\beta_9 \text{ Proportion Not Burnable}(\tau)\\
&+\beta_{11} \text{ Forest Connectivity by Burnable Cover }(\tau)\\
&+\beta_{12} \text{ Connectivity by Forest Cover }(\tau)\\
&+\beta_{13} \text{ Connectivity by Forest Cover} * \text{Mean Canopy Cover }(\tau)\\
&+\beta_{14} \text{ Connectivity by Forest Cover} * \text{Mean Canopy Cover}^2(\tau)
\end{aligned}
$$

We compared the modeled relationships of high-severity burn area to fuel availability and structure to a null model that assumed that variability in high-severity burn area was structurally unrelated to variability in fuel availability. The null model includes only an intercept term, as defined by:

$$Q_{high\text{-}severity\ burn\ area}(\tau = 0.95) = \beta_0(\tau)$$

Therefore, predictions from the null model are equivalent to the 95th percentile of high-severity burn area and do not vary with any of the fuel availability or structure variables.

Model coefficients and confidence intervals

To calculate confidence intervals of model coefficients, we calculated the coefficients for each variable using xy-pairs bootstrapping with 10,000 replications to generate a sample of coefficient estimates (Koenker 1994). We calculated the mean, the 2.5 percentile, and the 97.5 percentile of the 10,000 estimates.

Model responses and confidence intervals

To calculate the modeled responses to mean canopy cover, standard deviation in canopy cover, and forest connectivity by forest cover, we used the full model including 2020 fires to predict high-severity burned forest area and its 95% confidence intervals across the full range of each predictor variable, while holding all other predictor variables constant at their median values. We only modeled the responses for these three predictor variables because these were the predictor variables with coefficient confidence interval estimates that did not include zero. To evaluate the effect of the interaction between mean canopy cover and forest connectivity by forest cover on high-severity burn area, we used the full model to predict high-severity burn area and its 95% confidence intervals across the full range of forest connectivity by forest cover, while holding mean canopy cover constant at each of ten quantiles of mean canopy cover (0.05, 0.15, 0.25, 0.35, 0.45, 0.55, 0.65, 0.75, 0.85, and 0.95). All other variables were held constant at their median values. We generated predictions and confidence intervals from the null model across the full range of each predictor variable using the same process. However, because the null model did not

contain coefficient terms for any of the predictor variables, the predictions are constant with respect to each predictor variable.

High-severity burn area predictions and uncertainty

We used the model developed from fires that occurred from 2001 to 2020 to predict high-severity burn area and its confidence intervals for all 11,962 coniferous watersheds.

We used Bailey's ecoregions separated into the Nature Conservancy Terrestrial Ecoregions (Bailey 1998; Olson and Dinerstein 2002) to assess how high-severity burned forest area changed from including 2020 data varied according to ecoregion-level variation in climate. The Nature Conservancy Terrestrial Ecoregions are large land areas that contain distinct species assemblages and communities, and were determined based on synthesis of previous biogeographical research (Olson and Dinerstein 2002). These ecoregions are a common unit of analysis in studies of fire regimes and fire severity (Parks et al. 2018; Hessburg et al. 2019) and are available for public download at https://geospatial.tnc.org/. To allow for comparison of our results in the context of a previous framework of climate and fuel limitation across ecoregions in western North America and to enable plotting across a range of ecoregions, we only considered watersheds within the set of Bailey's ecoregions used by Hessburg et al. (2019), except for one ecoregion located in Mexico where LANDFIRE data is not available, resulting in 9994 coniferous forest watersheds in 18 unique ecoregions. For ecoregions that contained area in both the continental US and Canada or Mexico, we only considered watersheds within the continental United States where LANDFIRE data was available. We used long term (1958–2020) climatic water deficit as a proxy for the degree of climate vs. fuel limitation, with the assumption that lower climatic water deficit corresponds to higher climate limitation and lower aridity. Climatic water deficit is the difference between the potential evapotranspiration and the actual evapotranspiration (Stephenson 1990). It integrates the effects of temperature, humidity, and precipitation on fuel aridity (Abatzoglou and Williams 2016). We calculated mean climatic water deficit as the mean climatic water deficit from all monthly records from 1958 to 2020 from TerraClimate (Abatzoglou et al. 2018) in Google Earth Engine. To calculate the ecoregion-level mean climatic water deficit, we averaged the climatic water deficit over all 4 km pixels in the ecoregion.

Results

Across 3493 fires in watersheds, mean canopy cover, heterogeneity in canopy cover, and forest connectivity by forest had robust effects on high-severity burned area, measured as the 95th percentile of proportion of the forested area within the watershed that burned at high-severity. The 95% confidence intervals of the standardized coefficients of mean canopy cover, standard deviation in canopy cover, and forest connectivity by forest on high-severity burn area excluded zero (Fig. 2a).

Mean forest canopy cover, a proxy for fuel availability, had a strong positive effect on high-severity burn area within a watershed ($\beta_{\text{Mean canopy cover}} = 0.34$, 95% CI [0.25, 0.42], $\beta_{\text{Mean canopy cover}^2} = -0.12$, 95% CI [− 0.30, 0.06], Fig. 2, SI Figures Fig. S9). Heterogeneity in forest cover, a proxy for fuel discontinuity, had a negative effect on high-severity burn area ($\beta_{\text{SD canopy cover}} = -0.18$, 95% CI [− 0.25, − 0.1] and $\beta_{\text{SD canopy cover}^2} = -0.22$, 95% CI [− 0.33, − 0.03], Fig. 2, SI Figures Fig. S9). Forest connectivity by forest had a weak but robust positive effect on high-severity burn area ($\beta_{\text{Forest connectivity}} = 0.07$, 95% CI [0.02, 0.13], Fig. 2, SI Figures Fig. S9).

Predicted high-severity burn area varied substantially among the 11,962 coniferous forest HUC-12 watersheds in the western US (Fig. 3a). The percentage of the forested area predicted to burn at high-severity varied from 3 to 80%, and was highest for forests in the Pacific Northwest, the northern coast of California, and the Sierra Nevada (black colored watersheds in Fig. 3a). Watersheds with higher uncertainty in predicted high-severity burn area, specifically those with a 95% confidence interval size greater than 0.2, were concentrated in the West Cascades, the North Cascades, and the Pacific Northwest Coast (Fig. 3b, ecoregion names in Fig. 4b).

The Pacific Northwest is home to many regions characterized by cool, wet climate conditions that support productive forests with fire regimes that are usually climate-limited (Littell et al. 2009; Hessburg et al. 2019). In these systems, climate conditions that are conducive to widespread burning

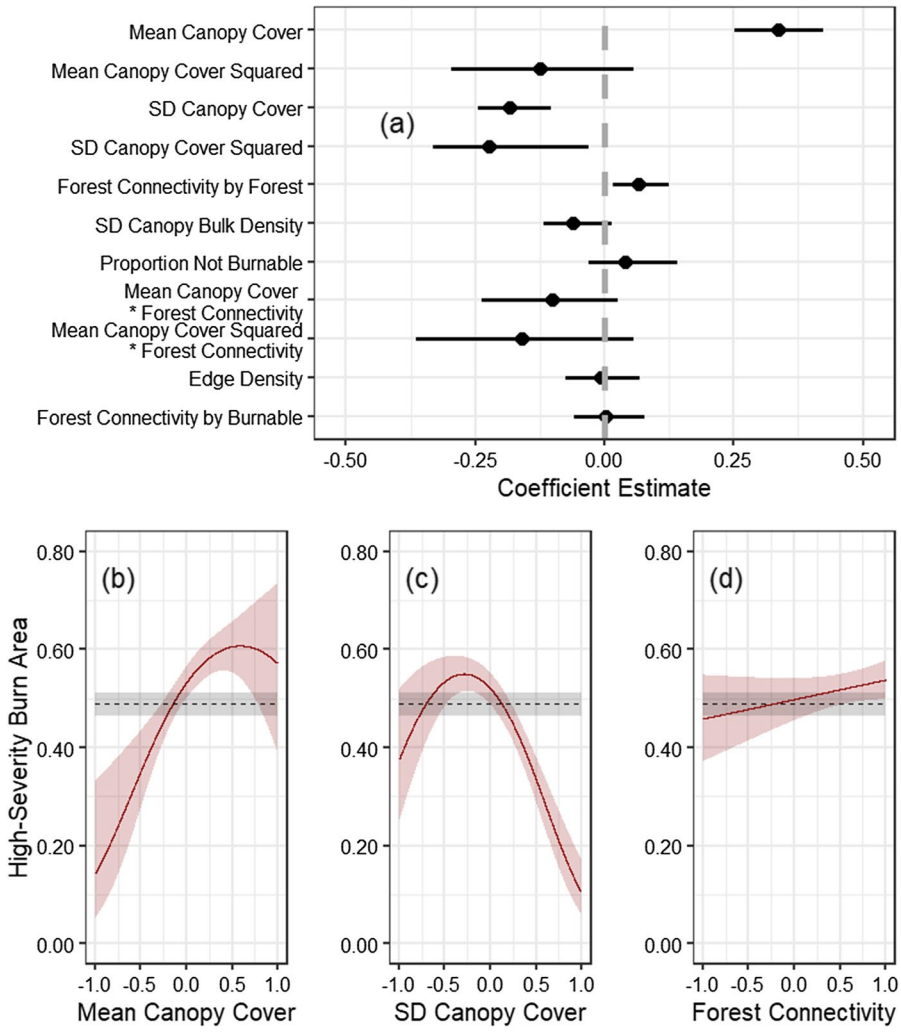

Fig. 2 Responses of the 95th percentile of high-severity burned forest area (referred to as high-severity burn area in the manuscript text) to forest fuel conditions from 2001 to 2020. The standardized coefficients and 95% confidence intervals for all variables included in the model (**a**), and (**b**–**d**) the predicted 95th percentile high-severity burned forest area on the y-axis, modeled as a function of each predictor variable (scaled) for which the 95% confidence interval of the standardized coefficient did not include zero: mean canopy cover (**b**), standard deviation in canopy cover (**c**), and forest connectivity (**d**). Gray dashed lines and gray shading shows the null model and 95% confidence intervals of the 95th percentile high-severity burned forest area, and red lines and red shading shows the predicted response and 95% confidence interval of the response of the 95th percentile of high-severity burned forest area to each scaled predictor variable

occur infrequently, but when they occur, the system is highly flammable due to the large amounts of fuel that accumulate during the long fire-free periods. During 2020, mesic forests in the Pacific Northwest were exposed to extreme fire conditions and several very large fires of spatial extents that were unprecedented in the contemporary record (Abatzoglou et al. 2021), but consistent with the historic fire regime of the region (Reilly et al. 2022). From 2001 to 2019, fuel-high-severity burn area relationships showed a condition where high canopy cover, which is common in the Pacific Northwest (SI Figures Fig. S4), was less capable of supporting large high-severity burn areas (Fig. 4a). Yet, in 2020, large high-severity burn areas occurred in these high canopy cover forests, particularly in climate-limited ecoregions of the Pacific Northwest (ecoregions with low climatic water deficit, shown as yellow and light orange points in Fig. 4b). However, exceptionally large high-severity burn areas also occurred in less climate-limited ecoregions (ecoregions with higher climatic water deficit are shown as purple and black points in Fig. 4b). Including the 2020 fires in the analysis changed the relationship between canopy cover and high-severity burn area by increasing high-severity burn area at high mean canopy cover values (Fig. 4b).

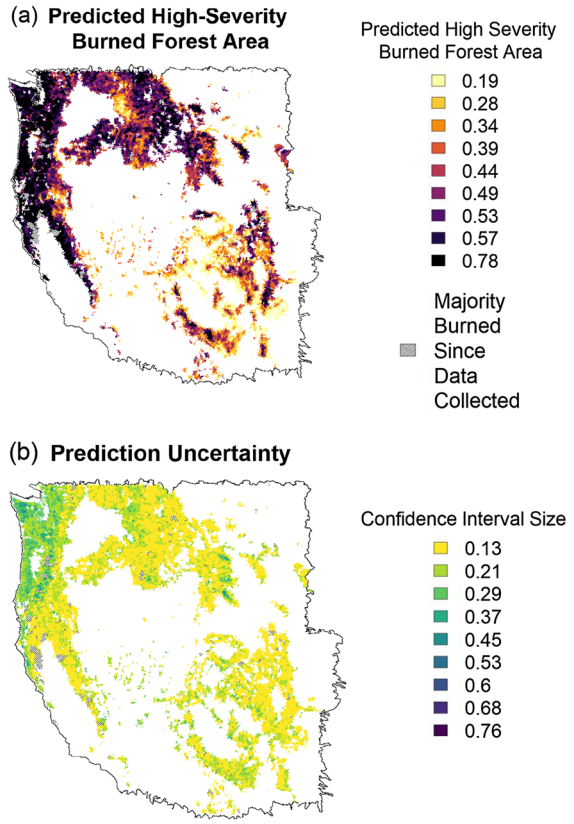

Fig. 3 The predicted 95th percentile of high-severity burned forest area and its uncertainty, as predicted from fuel availability and structure, varies among watersheds in the western US. Panels (**a**) and (**b**) show the predicted 95th percentile of proportion forest burned at high-severity in each watershed in the western US from the model. For the model predictions (**a**), the legend labels are the upper boundary, rounded to two decimal places, of each of ten quantiles of predicted 95th percentile of high-severity burned forest area predictions aggregated across predictions. For the uncertainty (**c**), the legend shows the upper boundary, rounded to two decimal places, of ten equally-spaced categories of 95% confidence interval size from the minimum to the maximum 95% confidence interval size. Watersheds with at least 50% of their area burned since the imagery was collected (2016–2020) are hashed. However, this data did not include fires from 2021 or 2022, therefore watersheds where more than 50% of the watershed burned during 2021 or 2022 are not classified here

Discussion

The increasing forest area burned at high-severity in recent forest wildfires (Parks and Abatzoglou 2020) threatens forest regeneration (Coop et al. 2020), wildlife habitat (Jones et al. 2016), and water resources (Williams et al. 2022). Recent studies have demonstrated the importance of fuel properties to the probability of high-severity fire at individual pixels (Parks et al. 2018; Koontz et al. 2020). However, wildfire is a contagious process where the area of forest with the potential to burn at high-severity depends on the availability and mosaic of fuel at multiple scales (Hagmann et al. 2021). Here, we demonstrate that forest area burned at high-severity at the HUC-12 watershed scale increases with increasing forest fuel availability and connectivity, and decreases with increasing forest cover heterogeneity in coniferous forest watersheds in the western US from 2001 to 2020. Our results suggest that in forests in the western US with fuel limited fire regimes, fuel treatments to decrease forest connectivity, increase heterogeneity, and reduce fuel availability could limit the forested area burned at high-severity within watersheds. In forests with usually climate-limited fire regimes, exceptionally high fuel availability increases the risk of large forest areas burned at high-severity when climate conditions are conducive to burning.

Forest area burned at high-severity increases with increasing fuel availability and connectivity and decreases with increasing heterogeneity

Mean canopy cover had a strong positive effect on high-severity burned area (Fig. 2), consistent with previous results that remotely-sensed estimates of fuel characteristics are strong predictors of the probability of high-severity fire at a single pixel from the western US (Parks et al. 2018) and that the probability of high-severity fire responds positively to NDVI in yellow pine and mixed-conifer forests in the Sierra Nevada (Koontz et al. 2020). Higher mean canopy cover is indicative of greater canopy fuel availability, which facilitates the spread of high-severity crown fires.

The relationship between tree crown connectivity and the potential transmission of crown fires is a fundamental concept in wildfire behavior modeling and fuel treatment planning (Agee and Skinner 2005; Ager et al. 2014; North et al. 2021) that has been demonstrated in field studies showing that greater canopy separation is associated with lower fire-induced tree mortality (North and Hurteau 2011; Safford et al. 2012). The positive response of high-severity burn area to forest connectivity by forest reported here (Fig. 2) provides observational evidence in

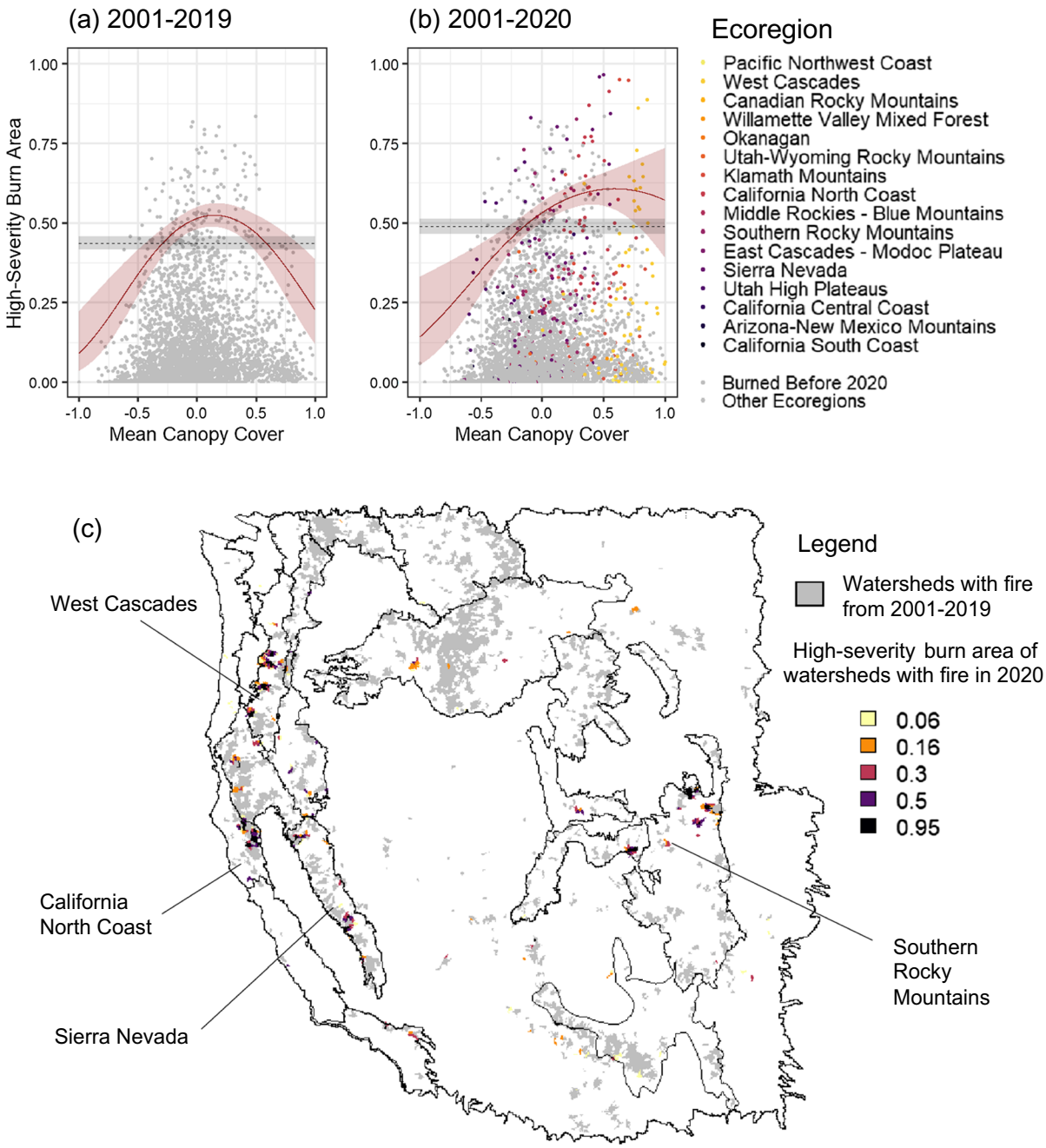

support of this fundamental concept over a larger spatial extent than previously studied. Although a variety of metrics have been developed to quantify forest landscape patterns related to connectivity (McGarigal and Marks 1995), we found that at the watershed-scale, the metric of forest connectivity that we developed specifically to account for wildfire behavior was more sensitive to the type of variation in forest connectivity expected to be relevant to wildfire propagation (Fig. S1), and was also a more robust predictor of high-severity burn area. Given that the controls on area burned vary as a function of scale (i.e., top-down controls at regional scales and bottom-up controls at local scales, Heyerdahl et al. 2001) and that the sensitivity of wildfire spread to fuel continuity can be diminished depending on fire behavior, the scale at

◂**Fig. 4** Watersheds with high canopy cover had larger high-severity burn areas during the 2020 fire season. Gray and colored points show the data from 2001 to 2019 (**a**) and 2001–2020 (**b**), where fires that occurred in 2020 and are within the ecoregions analyzed by Hessburg et al. 2019 are colored. The predicted 95th percentile of the proportion of forested area burned at high-severity (red lines) and 95% confidence intervals (red shading) as a function of mean canopy cover (scaled) when only data from 2001 to 2019 is included in the model (**a**), and when data including fires from 2020 are included in the model (**b**), show the increase in predicted forest area burned at high-severity for the watersheds with the highest mean canopy cover. Gray dashed lines and gray shading shows the null model and 95% confidence intervals of the 95th percentile high-severity burned forest area for each of the time periods. In (**b**), points are colored according to the Bailey's climatic ecoregions analyzed in Hessburg et al. (2019), ordered according to increasing long-term climatic water deficit as a proxy for relative climate limitation on fire, where lower climatic water deficit corresponds to greater climate limitation on fire. Panel (**c**) shows the ecoregion boundaries (black outlines) with the four ecoregions with the greatest number of fires added in 2020 labeled. Watersheds with fire in 2001–2019 are shown in gray, and watersheds with fire in 2020 are colored according to their high-severity burn area. For high-severity burn area in (**c**), the legend labels are the upper boundary, rounded to two decimal places, of each of six quantiles of high-severity burned forest area of fires that occurred in 2020

which fuel continuity is evaluated should change with the scale at which fire is being evaluated. Since much of our understanding of fire was developed in the linear part of a nonlinear system (Juang et al. 2022), we may start finding that even at fine scales, patterns that used to explain fire spread are less effective as changing climate drives increasingly extreme wildfire behavior. This is an area that requires active investigation as the amount of empirical data on extreme wildfires increases.

There are a number of metrics for measuring landscape configuration which have been developed to incorporate insights from a range of disciplines (McGarigal and Marks 1995; Urban and Keitt 2001; Frazier 2019). However, many of these metrics are correlated with each other and vary along a gradient of adjacency (Neel et al. 2004), and as such their need has been questioned (2019). Others have argued that although metrics are correlated, the subtle differences lend themselves to different applications (Neel et al. 2004), and that metrics used in individual studies should be carefully chosen according to the objectives of the study (Gustafson 2019). The forest connectivity metric we used in this study calculates the average proportion of the total forest area that is connected to each pixel, and is therefore directly susceptible to catching wildfire if an individual pixel was burning at high-severity. Although the forest connectivity metric was correlated, to varying degrees, with the alternative metrics of landscape configuration (Pearson R Correlation Coefficients were 0.7, − 0.48, and 0.16 for proportion of like adjacency, edge density, and patch density respectively, SI Tables Table S2), analyses of the behavior of alternative metrics of configuration on hypothetical forest cover patterns clearly demonstrate that the existing metrics do not capture the important differences in very distinct spatial patterns (Fig. S1a, S1b). Furthermore, the forest connectivity metric we developed was a stronger predictor of high-severity burn area than the other adjacency metrics at the scale of forest watersheds in the western US (Fig. 2a, Supporting Information Table S3). It is possible that alternative approaches for quantifying connectivity to high-severity fire may be effective at different spatial extents and grain sizes. For example, graph theory offers a range of metrics for quantifying landscape connectivity, including incorporating the distance among patches into the calculation of connectivity (Urban and Keitt 2001). However, the distance between patches that results in high-severity fire connectivity varies significantly depending on fire behavior, while distance-based calculations add to computational intensity (Moilanen 2011). Thus, connectivity metrics from graph theory were not the best trade-off between computational tractability and ecological informativeness at the scale of our analyses, which covered 11,962 landscapes (watersheds), that each had many tens of thousands of pixels. However, metrics from graph theory may be able to effectively quantify additional elements of landscape connectivity for wildfire applications in analyses at a different combination of grain size and extent (e.g. Aparício et al. 2022). At the watershed-scale, our metric of forest connectivity is capable of representing the range of observed conditions, is more strongly correlated with the response variable than the other metrics of landscape configuration, and is based on first principles of wildfire behavior, meeting three of the four criteria for a good metric specified by Riitters (2019). Evaluating this metric in other discipline-specific contexts will determine if it meets the fourth criterion.

Heterogeneity in canopy cover within a watershed had a relatively strong negative effect on forest area

burned at high-severity—at the midpoint of the standard deviation in canopy cover predicted high-severity burn area was 0.53, whereas at the maximum standard deviation in canopy cover, predicted high-severity burn area was 0.12 (Fig. 2). These results are consistent with Koontz et al. (2020) who found that in Sierra Nevada yellow pine and mixed-conifer forests, single pixels with higher heterogeneity (measured by standard deviation) in NDVI within their immediate neighborhood had a lower probability of high-severity fire. Higher spatial heterogeneity in forest cover indicates high variability in forest canopy cover within the forested area watershed (SI Figures Fig. S2), which may be associated with patches within landscapes with insufficient forest fuel densities to maintain the spread of high-severity crown fire across large landscapes. The results we present extend the findings of Koontz et al. (2020) from coniferous forests in the Sierra Nevada to coniferous forests across the western US and further show that higher fuel heterogeneity is associated with not only a lower probability of high-severity fire in individual locations (Koontz et al. 2020), but also with smaller high-severity burn areas within coniferous forest watersheds.

Fuel availability and high-severity burn area relationships with 2020 highlight risks to climate-limited systems

Fire regimes in western US forests vary along a gradient of climate-limited to fuel-limited (Littell et al. 2009; Hessburg et al. 2019). The consistency of the hump-shaped relationship between mean canopy cover and high-severity burn area from 2001 to 2019 (Fig. 4a) and the hypothesized and observed hump-shaped relationship between fire activity and aridity/productivity at the global scale (the intermediate fire-productivity hypothesis, Pausas and Paula 2012; Pausas and Ribeiro 2013), demonstrates that coniferous forest watersheds in the western US cover a wide range of aridity/productivity and corresponding fire regimes. These findings from 2001 to 2019 fires are consistent with the notion that forests with the highest mean canopy cover in our analysis have primarily climate-limited fire regimes and that fuel has a relatively weak influence on the area burned at high-severity in these systems (Littell et al. 2009; Krawchuk and Moritz 2011).

In 2020, widespread high-severity burning was observed across fuel and climate-limited systems in the western US (Higuera et al. 2021; Reilly et al. 2022; Safford et al. 2022), and globally (Boer et al. 2020; Talucci et al. 2022). Somewhat surprisingly, including the 2020 fires changed the relationship between mean canopy cover and high-severity burn area by increasing high-severity burn area in forests with the highest mean canopy cover (Fig. 4b). If the 2020 fires were simply interpreted as an extreme climate/fire weather event alone, then we would have expected increased high-severity burning regardless of fuel conditions. However, fires that occurred during 2020 in forests with low fuel availability (lower than the midpoint of mean canopy cover) had high-severity burn areas that were within the range of high-severity burn areas that had been observed prior to 2020, whereas forests with high fuel availability (higher than the midpoint of mean canopy cover) had high-severity burn areas that were larger than had been observed prior to 2020 (Fig. 4b). When fire weather conditions are conducive to burning, these high mean canopy cover forests can support substantial proportions of high-severity fire.

Climate change has increased fuel aridity in western US forests (Abatzoglou and Williams 2016), in both climate-limited and fuel-limited systems (Rupp et al. 2017). In climate-limited systems, reduced climatic barriers to wildfire, specifically elevated fuel aridity (Higuera and Abatzoglou 2020; Higuera et al. 2021), or exceptional combinations of fuel aridity and wind speed (Abatzoglou et al. 2021) were important drivers of increased high-severity burning in 2020. Although unprecedented in the contemporary record, the climatic conditions and size and severity of the 2020 fires in the western Cascades are consistent with the historic fire regimes in the region (Reilly et al. 2022). However, climate change could increase the frequency of the historically infrequent conditions that are conducive to burning in climate-limited systems in the western US, including the Pacific Northwest (Higuera and Abatzoglou 2020; Higuera et al. 2021). Increasing aridity has an exponential effect on area burned because aridity enables larger fires and larger fires have greater potential for growth (Juang et al. 2022), and the additional fuel drying due to increased atmospheric water demand can increase the amount of energy available for release during

combustion (Goodwin et al. 2021). In the absence of changes in the frequency of extreme strong wind events, increasing aridity driven by climate change would increase the likelihood of extreme combinations of strong winds and fuel aridity, such as those that occurred during the 2020 fire year. The high-severity fire proportions in the fires that occurred in the western Cascades in 2020 during the period of high aridity but normal wind speeds were within the range of high-severity fire proportion in Pacific Northwest fires between 1984 and 2010, suggesting that wind speed was an important driver of the area burned at high-severity (Reilly et al. 2017; Evers et al. 2022). However, an increase in the frequency of periods with high fuel aridity could also allow for an increase in fire frequency, and if individual fires burned with the same proportion high-severity as fires that occurred from 1984 to 2010, an increase in the frequency of those fires would result in an increase in the frequency of high-severity fire.

Recent modeling studies evaluating the vulnerability of forest carbon to wildfire across the western US have classified forests in the Pacific Northwest as low risk relative to other regions, possibly because these models combine fuel conditions and climate in the calculation of risk (Buotte et al. 2018), and other regions of the western US are projected to be exposed to climate conditions conducive to fire with greater frequency. The results we present here including the 2020 fires across the western US suggest that mesic forests of the Pacific Northwest and other climate-limited systems are at greater risk of large high-severity burn areas when fuel and weather conditions allow. If the extreme climatic conditions observed in 2020 conducive to burning occur more frequently, as expected (Higuera and Abatzoglou 2020; Coop et al. 2022) watersheds in climate-limited regions could be exposed to the potential for large proportions of their forested area to burn at high-severity with increasing frequency. In a background of ongoing aridification, in comparison with fuel-limited systems in the western US, the high fuel availability of usually climate-limited forests could partially offset the reduction in potential high-severity burn area that results from their relatively lower frequency of exposure to climate conditions that are conducive to fire.

Conclusions

Here, we show that coniferous forested watersheds in the western US with higher connectivity in forest cover, lower forest cover heterogeneity, and higher fuel availability have larger high-severity burn areas during recent wildfires. Prior to 2020, watersheds with the highest fuel availability, located in mesic forests in the Pacific Northwest, had small to intermediate high-severity burn areas, but had multiple very large high-severity burn areas during 2020. Our results identify forested watersheds where fuel conditions contribute to a high risk of large high-severity forest wildfires, and suggest that in forests with fuel-limited fire regimes, fuel management could mitigate the risk of large high-severity burns by reducing fuel accumulation and forest connectivity, and increasing forest cover heterogeneity (North et al. 2021). The change in the relationships between fuel and high-severity burn area from including 2020 fires suggests that the exceptionally high fuel availability in forests with usually climate-limited fire regimes in the Pacific Northwest corresponds to a uniquely high sensitivity to climate conditions that are an inadequate barrier to wildfire.

Author contributions EJF, BMC, and MDH designed research, EJF, PP, and ZLS performed research, EJF analyzed data, EJF, BMC, ZLS, and MDH wrote the paper. All authors reviewed the manuscript and approved publication.

Funding EJF and MDH acknowledge support from the University of New Mexico, the Interagency Carbon Cycle Science program Grant no. 2017-67004-26486/Project accession no. 1012226 from the USDA National Institute of Food and Agriculture, and the Environmental Defense Fund.

Data availability All data used in the analysis are openly available. Existing Vegetation Cover, Canopy Bulk Density, and 40 Scott and Burgan Fire Behavior Fuel Model data are available from the LANDFIRE program (https://landfire.gov/, 34). The HUC-12 watershed boundary dataset is available from The National Map (https://apps.nationalmap.gov/). Fire perimeters from 2001 to 2019 are available from the Monitoring Trends in Burn Severity (MTBS) program (https://www.mtbs.gov/, Eidenshink et al. 2007). Fire perimeters for 2020 fires are available from the Fire Event Delineation (https://scholar.colorado.edu/concern/datasets/8336h304x, St. Denis et al. 2022). Fire severity data were derived using publicly available code and model training data (https://tinyurl.com/CBImodel) from Parks et al. (2019). Climatic water deficit data are available from TerraClimate (https://www.climatologylab.org/datasets.html, Abatzoglou et al. 2018). Bailey's ecoregions separated into the Nature Conservancy Terrestrial Ecoregions are

available from the Nature Conservancy Geospatial Conservation Atlas (https://geospatial.tnc.org/; Bailey 1998; Olson and Dinerstein 2002). The code used to perform the analyses and the derivative datasets are available at: https://doi.org/10.5061/dryad.qrfj6q5k7.

Declarations

Competing interests The authors declare no competing interests.

References

Abatzoglou JT, Williams AP (2016) Impact of anthropogenic climate change on wildfire across western US forests. Proc Natl Acad Sci USA 113(42):11770–11775

Abatzoglou JT, Dobrowski SZ, Parks SA, Hegewisch KC (2018) TerraClimate, a high-resolution global dataset of monthly climate and climatic water balance from 1958–2015. Sci Data 5:170191

Abatzoglou JT, Rupp DE, O'Neill LW, Sadegh M (2021) Compound extremes drive the western Oregon wildfires of September 2020. Geophys Res Lett 48:e2021GL092520

Agee JK, Skinner CN (2005) Basic principles of forest fuel reduction treatments. For Ecol Manag 211:83–96

Ager AA, Day MA, Finney MA, Vance-Borland K, Vaillant NM (2014) Analyzing the transmission of wildfire exposure on a fire-prone landscape in Oregon, USA. For Ecol Manag 334:377–390

Aparício BA, Pereira JMC, Santos FC, Bruni C, Sá ACL (2022) Combining wildfire behavior simulations and network analysis to support wildfire management: a Mediterranean landscape case study. Ecol Indic 137:108726

Bailey RG (1998) Ecoregions map of North America: explanatory note. USDA-FS, Washington

Balch JK, St.Denis LA, Mahood AL, Mietkiewicz NP, Williams TM et al (2020) FIRED (Fire Events Delineation): an open, flexible algorithm and database of US fire events derived from the MODIS Burned Area product (2001–2019). Remote Sens 12(21):3498

Beck WM (2019) Package 'WRTDStidal.' https://cran.r-project.org/web/packages/WRTDStidal/index.html

Bladon KD, Emelko MB, Silins U, Stone M (2014) Wildfire and the future of water supply. Environ Sci Technol 48:8936–8943

Boer MM, Resco de Dios V, Bradstock RA (2020) Unprecedented burn area of Australian mega forest fires. Nat Clim Change 10:171–172

Bottai M, Cai B, McKeown RE (2010) Logistic quantile regression for bounded outcomes. Stat Med 29:309–317

Bowman DMJS, Balch JK, Artaxo P, Bond WJ, Carlson JM et al (2009) Fire in the earth system. Science 324:481–484

Buotte PC, Levis S, Law BE, Hudiburg TW, Rupp DE et al (2018) Near-future forest vulnerability to drought and fire varies across the western United States. Glob Change Biol 25:290–303

Burke M, Driscoll A, Heft-Neal S, Xue J, Burney J et al (2021) The changing risk and burden of wildfire in the United States. Proc Natl Acad Sci USA 118(2):e2011048118

Coop JD, Parks SA, Stevens-Rumann CS, Crausbay SD, Higuera PE et al (2020) Wildfire-driven forest conversion in western North American landscapes. Bioscience 70:659–673

Coop JD, Parks SA, Stevens-Rumann CS, Ritter SM, Hoffman CM (2022) Extreme fire spread events and area burned under recent and future climate in the western USA. Glob Ecol Biogeogr 31:1949–1959

Dahlin K, Asner GP, Field CB (2013) Environmental and community controls on plant canopy chemistry in a Mediterranean-type ecosystem. Proc Natl Acad Sci USA 110(17):6895–6900

Eidenshink J, Schwind B, Brewer K, Zhu Z-L, Quayle B et al (2007) A project for monitoring trends in burn severity. Fire Ecol 3:3–21

Evers C, Holz A, Busby S, Nielsen-Pincus M (2022) Extreme winds alter the influence of fuels and topography on megafire burn severity in season temperate rainforests under record fuel aridity. Fire 5(2):41

Frazier AE (2019) Emerging trajectories for spatial pattern analysis in landscape ecology. Landsc Ecol 34:2073–2082

Goodwin MJ, Zald HS, North MP, Hurteau MD (2021) Climate-driven tree mortality and fuel aridity increase wildfire's potential heat flux. Geophys Res Lett 48(24):e2021GL094954

Guo Q, Cade BS, Dawson W, Essl F, Kreft H et al (2021) Latitudinal patterns of alien plant invasions. J Biogeogr 48(2):253–262

Gustafson EJ (1998) Quantifying landscape spatial pattern: what is the state of the art? Ecosystems 1:143–156

Gustafson EJ (2019) How has the state-of-the-art for quantification of landscape pattern advanced in the twenty-first century? Landsc Ecol 34:2065–2072

Hagmann RK, Hessburg PF, Prichard SJ, Povak NA, Brown PM et al (2021) Evidence for widespread changes in the structure, composition, and fire regimes of western North American forests. Ecol Appl 31(8):e02431

Hessburg PF, Churchill DJ, Larson AJ, Haugo RD, Miller C et al (2015) Restoring fire-prone Inland Pacific landscapes: seven core principles. Landsc Ecol 30:1805–1835

Hessburg PF, Miller CL, Parks SA, Povak NA, Taylor AH et al (2019) Climate, environment, and disturbance history govern resilience of Western North American Forests. Front Ecol Evol 7:239

Hessburg PF, Prichard SJ, Hagmann RK, Povak NA, Lake FK (2021) Wildfire and climate change adaptation of western North American forests: a case for intentional management. Ecol Appl. https://doi.org/10.1002/eap.2432

Hesselbarth MHK, Sciani M, With KA, Wiegand K, Nowosad J (2019) *landscapemetrics*: an open-source R tool to calculate landscape metrics. Ecography 42(10):1648–1657

Heyerdahl EK, Brubaker LB, Agee JK (2001) Spatial controls of historical fire regimes: a multi-scale example from the Interior West, USA. Ecology 82:660–678

Higuera PE, Abatzoglou JT (2020) Record-setting climate enabled the extraordinary 2020 fire season in the western United States. Glob Change Biol 27(1):1–2

Higuera PE, Shuman BN, Wolf KD (2021) Rocky Mountain subalpine forests now burning more than any time in recent millennia. Proc Natl Acad Sci USA 118:e2103135118

Jaffe MR, Collins BM, Levine JI, Northrop H, Malandra F, Hurteau MD, Stephens SL, North M (2021) Prescribed fire shrub consumption in a Sierra Nevada mixed-conifer forest. Can J For Res 51:1718–1725

Jones GM, Gutiérrez RJ, Tempel DJ, Whitmore SA, Berigan WJ et al (2016) Megafires: an emerging threat to old-forest species. Front Ecol Environ 14(6):300–306

Juang CS, Williams AP, Abatzoglou JT, Balch JK, Hurteau MD et al (2022) Rapid growth of large forest fires drives the exponential response of annual forest-fire area to aridity in the western United States. Geophys Res Lett 49:e2021GL097131

Koenker RW (1994) Confidence intervals for regression quantiles. In: Mandl P, Huskova M (eds) Asymptotic statistics. Springer, New York, pp 349–359

Koenker R (2018) Package 'quantreg'. https://cran.r-project.org/web/packages/quantreg/index.html

Koenker R, Bassett G (1978) Regression quantiles. Econometrica 46(1):33–50

Koenker R, Hallock KF (2001) Quantile regression. J Econ Perspect 15(4):143–156

Koenker R, Machado JAF (2012) Goodness of fit and related inference processes for quantile regression. J Am Stat Assoc 94(448):1296–1310

Koo E, Pagni PJ, Weise DR, Woycheese JP (2010) Firebrands and spotting ignition in large-scale fires. Int J Wildland Fire 19:818–843

Koontz MJ, North MO, Werner CM, Fick SE, Latimer AM (2020) Local forest structure variability increases resilience to wildfire in dry western U.S. coniferous forests. Ecol Lett 23(3):483–494

Krawchuk MA, Moritz MA (2011) Constraints on global fire activity vary across a resource gradient. Ecology 92(1):121–132

Littell JS, McKenzie D, Peterson DL, Westerling AL (2009) Climate and wildfire area burned in western US ecoprovinces, 1916–2003. Ecol Appl 19(4):1003–1021

Liu JC, Mickley LJ, Sulprizio MP, Dominci F, Yue X et al (2016) Particulate air pollution from wildfires in the Western US under climate change. Clim Change 138(3):655–666

McGarigal K, Marks BJ (1995) FRAGSTATS: spatial analysis program for quantifying landscape structure. USDA Forest Service General Technical Report PNW-GTR-351

McGarigal K, Cushman SA, Ene E (2012) FRAGSTATS v4: spatial pattern analysis program for categorical and continuous maps. Computer software program produced by the authors at the University of Massachusetts, Amherst

McLaughlan KK, Higuera PE, Miesel JR, Rogers BM, Schweitzer J et al (2020) Fire as a fundamental ecological process: research advances and frontiers. J Ecol 108:2047–2069

Miller JD, Knapp EE, Key CH, Skinner CN, Isbell C et al (2009) Calibration and validation of the relative differenced Normalized Burn Ratio (RdNBR) to three measures of fire severity in the Sierra Nevada and Klamath Mountains, California, USA. Remote Sens Environ 113:645–656

Moilanen A (2011) On the limitations of graph-theoretic connectivity in spatial ecology and conservation. J Appl Ecol 48:1543–1547

Neel MC, McGarigal K, Cushman SA (2004) Behavior of class-level landscape metrics across gradients of class aggregation and area. Landsc Ecol 19:435–455

North MP, Hurteau MD (2011) High-severity wildfire effects on carbon stocks and emissions in fuels treated and untreated forest. For Ecol Manag 261(6):1115–1120

North MP, York RA, Collins BM, Hurteau MD, Jones GM et al (2021) Pyrosilviculture needed for landscape resilience of dry western United States forests. J For 119(5):520–544

Olson DM, Dinerstein E (2002) The global 200: priority ecoregions for global conservation. Ann Missouri Bot Gard 199–224

Parks SA, Abatzoglou JT (2020) Warmer and drier fire seasons contribute to increases in area burned at high-severity in western US forests from 1985 to 2017. Geophys Res Lett 47:e2020GL089858

Parks SA, Holsinger LM, Panunto MH, Jolly WM, Dobrowski SZ et al (2018) High-severity fire: evaluating its key drivers and mapping its probability across western US forests. Environ Res Lett 13:044037

Parks SA, Holsinger LM, Koontz MJ, Collins L, Whitman E et al (2019) Giving ecological meaning to satellite-derived fire severity metrics across North American forests. Remote Sens 11:1735

Pausas JG, Keeley JE (2019) Wildfires as an ecosystem service. Front Ecol Environ 17:289–295

Pausas JG, Paula S (2012) Fuel shapes the fire-climate relationship: evidence from Mediterranean ecosystems. Glob Ecol Biogeogr 21(11):1074–1082

Pausas JG, Ribeiro E (2013) The global fire-productivity relationship. Glob Ecol Biogeogr 22:728–736

Prichard SJ, Povak NA, Kennedy MC, Peterson DW (2020) Fuel treatment effectiveness in the context of landform, vegetation, and large, wind-driven wildfires. Ecol Appl 30:e02104

Reeves MC, Ryan KC, Rollins MG, Thompson TG (2009) Spatial fuel data products of the LANDFIRE project. Int J Wildland Fire 18:250–267

Reilly MJ, Dunn CJ, Meigs G, Spies TA, Kennedy RE et al (2017) Contemporary patterns of fire extent and severity in forests of the Pacific Northwest, USA (1985–2010). Ecosphere 8:e01695

Reilly MJ, Zuspan A, Halofsky JS, Raymond C, McEvoy A et al (2022) Cascadia burning: the historic, but not historically unprecedented, 2020 wildfires in the Pacific Northwest, USA. Ecosphere 13:e4070

Rhoades CC, Nunes JP, Silins U, Doerr SH (2019) The influence of wildfire on water quality and watershed processes: new insights and remaining challenge. Int J Wildland Fire 28:721–725

Riitters K (2019) Pattern metrics for a transdisciplinary landscape ecology. Landsc Ecol 34:2057–2063

Rollins MG (2009) LANDFIRE: a nationally consistent vegetation, wildland fire, and fuel assessment. Int J Wildland Fire 18:235–249

Rupp DE, Li S, Mote PW, Shell KM, Massey N, Sparrow SN et al (2017) Seasonal spatial patterns of projected anthropogenic warming in complex terrain: a modeling study of the western US. Clim Dyn 48(7–8):2191–2213

Safford HD, Stevens JT, Merriam K, Meyer MD, Latimer AM (2012) Fuel treatment effectiveness in California yellow pine and mixed conifer forests. For Ecol Manag 274:17–28

Safford HD, Paulson AK, Steel ZL, Young DJN, Wayman RB (2022) The 2020 California fire season: a year like no other, a return to the past or a harbinger of the future? Glob Ecol Biogeogr 00:1–21

Scott J, Burgan R (2005) Standard fire behavior fuel models: a comprehensive set for use with Rothermel's surface fire spread model. USDA Forest Service, Rocky Mountain Research Station, General Technical Report RMRS-GTR-153, p 72

Sofaer HR, Jarnevich CS, Buchholtz EK, Cade BS, Abatzoglou JT, Aldridge CL, Comer PJ, Manier D, Parker LE, Heinrichs JA (2022) Potential cheatgrass abundance within lightly invaded areas of the Great Basin. Landsc Ecol 37:2607–2618

St. Denis LA, McGlinchy J, Mietkiewicz NP, Lindrooth EJ, Williams T, Cook MC, Mahood AL (2022) FIRED US CANADA Data Set. CIRES Earth Lab. https://scholar.colorado.edu/concern/datasets/8336h304x

Steel ZL, Safford HD, Viers JH (2015) The fire frequency-severity relationship and the legacy of fire suppression in California forests. Ecosphere 6:1–23

Steel ZL, Koontz MJ, Safford HD (2018) The changing landscape of wildfire: burn pattern trends and implications for California's yellow pine and mixed conifer forests. Landsc Ecol 33:1159–1176

Steel ZL, Foster D, Coppoletta M, Lydersen JM, Stephens SL et al (2021) Ecological resilience and vegetation transition in the face of two successive large wildfires. J Ecol 00:1–16

Stephens SL, Fulé PZ (2005) Western pine forests with continuing frequent fire regimes: possible reference sites for management. J For 103(7):357–362

Stephens SL, Moghaddas JJ, Edminster C, Fiedler CE, Haase S et al (2009) Fire treatment effects on vegetation structure, fuels, and potential fire severity in western U.S. forests. Ecol Appl 19(2):305–320

Stephens SL, Bernal AA, Collins BM, Finney MA, Lautenberger C, Saah D (2022) Mass fire behavior created by extensive tree mortality and high tree density not predicted by operational fire behavior models in the southern Sierra Nevada. For Ecol Manag 518:120258

Stephenson N (1990) Climatic control of vegetation distribution: the role of water balance. Am Nat 135(5):649–670

Stevens JT, Collins BM, Miller JD, North MP, Stephens SL (2017) Changing spatial patterns of stand-replacing fire in California conifer forests. For Ecol Manag 406:28–36

Stowell JD, Geng G, Saikawa E, Chang HH, Fu J et al (2019) Associations of wildfire smoke $PM_{2.5}$ exposure with cardiorespiratory events in Colorado 2011–2014. Environ Int 133:105151

Talucci AC, Loranty MM, Alexander HD (2022) Siberian taiga and tundra fire regimes from 2001–2020. Environ Res Lett 17:025001

Urban D, Keitt T (2001) Landscape connectivity: a graph-theoretic perspective. Ecology 82:1205–1218

U.S. Geological Survey and U.S. Department of Agriculture, Natural Resources Conservation Service (2013) Federal standards and procedures for the National Watershed Boundary Dataset (WBD), 4 ed. U.S. Geological Survey techniques and methods 11–A3, p 63. https://pubs.usgs.gov/tm/11/a3/

Williams AP, Livneh B, McKinnon KA, Hansen WD, Mankin JS et al (2022) Growing impact of wildfire on western US water supply. Proc Natl Acad Sci USA 119(10):e2114069119

Zhu Z, Ohlen D, Kost J, Chen X, Tolk B (2006) Mapping existing vegetation composition and structure for the LANDFIRE Prototype Project. In: Rollins MG, Frame CK (eds) The LANDFIRE Prototype Project: Nationally Consistent and Locally Relevant Geospatial Data and Tools for Wildland Fire Management. USDA Forest Service, Rocky Mountain Research Station, General Technical Report RMRS-GTR-175, Fort Collins, CO